Progress in Organic Coatings 174 (2023) 107279

Contents lists available at ScienceDirect

Progress in Organic Coatings

journal homepage: www.elsevier.com/locate/porgcoat

Modeling surface segregation of smart PU coatings at hydrophilic and hydrophobic interfaces via coarse-grained molecular dynamics and mesoscopic simulations

Deniz Kizilkaya [a,1], Hassan Ghermezcheshme [b,1], Sepide Eslami Sabzevar [b], Hesam Makki [b,c,*], Gokhan Kacar [a,**]

[a] Department of Genetics and Bioengineering, Faculty of Engineering, Trakya University, 22030 Edirne, Turkey
[b] Department of Polymer and Color Engineering, Amirkabir University of Technology, 424 Hafez Ave., Tehran, Iran
[c] Department of Chemistry, University of Liverpool, Liverpool L69 7ZD, UK

ARTICLE INFO

Keywords:
Smart coating
Polyurethane network
Surface responsive coatings
MARTINI model
DPD simulation

ABSTRACT

Developing adaptive coatings having desired functionalities at targeted interfaces is one of the major efforts in the coatings science area. The adaptation of the surface functionality to the changing surface conditions can be maintained by introducing dangling chains with different properties to the cross-linked polymer coatings. In this work, we strive to investigate the change in interfacial morphology of PU coatings as exposed to hydrophilic (HPI) and hydrophobic (HPB) interfaces by employing molecular simulations at the coarse-grained and mesoscopic levels. The molecular structure and surface segregation dynamics are studied for PU coatings having pure HPI, mixture of HPI and HPB, and amphiphilic dangling chains. The dual-scale simulations, Dissipative Particle Dynamics (DPD) and MARTINI model, yield results about the dangling chain structures at the interface in terms of their end-to-end distances, where HPI chains adopt a more extended conformation in water in comparison to oil interfaces. The reverse is observed to be valid for the HPB chains. Regarding the dangling chain dynamics, a swift migration towards the interfaces is noticed at about 10 ns for both of the simulation methods. The structures of the dangling chains and their interaction with the interfaces are also characterized by computing the radial distribution function (RDF) profiles. Preferential interactions between the HPI/water and HPB/oil are clearly noted. The switchability of the surfaces is also studied by simulating the system in cycles, such that the interface is changed from water to oil and back to water. The migration of HPI groups in the dangling chains towards water and vice versa in each cycle is clearly shown by the simulations. In all, the inherent structure and dynamics of the dangling chains is obtained at the molecular level by the dual-scale molecular simulations. Our findings reveal a significant level of understanding about interfacial morphology of thermoset coatings modified by dangling chains, where the results can be extended to find applications in guiding the experimental studies.

1. Introduction

The invention of the polyurethane (PU) in 1937 by Otto Bayer, has led to an emerging field of this material [1]. The resistance to abrasion, impact and weather durability, a wide range of mechanical properties, and tunable interfacial characteristics make PU a versatile material in many application areas such as foams, composites, sealants [2], coatings [3], hydrogels [4], contact lenses, and medical devices [5].

Polyurethanes are generally synthesized from the reaction between diisocyanates and polyols [6]. In general, a 3D cross-linked PU system can be realized by using components with an average functionality of more than two. It is also possible to incorporate a component with one functionality to build up a network with dangling chains. Dangling chains in the PU network show faster dynamics and a larger mobility range as compared to polymer chains that are connected from both sides to the network. As a result of the versatility of PU materials due to high compatibility and availability of reactive groups, conventional PU coatings can be equipped with dangling chains to present 'smart'

* Correspondence to: H. Makki, Department of Chemistry, University of Liverpool, Liverpool L69 7ZD, UK.
** Corresponding author.
E-mail addresses: h.makki@liverpool.ac.uk (H. Makki), gokhankacar@trakya.edu.tr (G. Kacar).
[1] These authors contributed equally to the manuscript.

https://doi.org/10.1016/j.porgcoat.2022.107279
Received 26 April 2022; Received in revised form 8 October 2022; Accepted 18 October 2022
Available online 27 October 2022

behavior so that it acquires the ability to switch its functionality as a result of changing its environment. The presence of dangling chains is observed to influence the surface molecular mobility [7], yield anti-biofouling surfaces [8,9], and increase the lubricious behavior [10,11]. Moreover, PU coatings with dangling chains are also observed to result in self-replenishing [12–16] and self-healing properties with improved thermal and mechanical properties [17].

In the current work, we explore the programmable functionality of a series of smart PU coatings that can change their surface functionality, i.e., hydrophilicity and hydrophobicity, upon presence of polar (liquid water or high relative humidity conditions) and apolar (oil) environments. The PU coatings are modified by HPI, HPB, and amphiphilic dangling chains in different configurations. The presence of a polar environment leads to the migration of the HPI (or HPI part of the) dangling chains, that are being present in the bulk of the coatings to the water interface and results in a HPI surface, while the HPB (or HPB part of the) dangling chains show a similar behavior at the polymer/oil (apolar environment) interface. Therefore, a series of smart coatings with a dynamic and programmable surface functionality (as a function of the environment) is proposed and the switchability of coatings equipped with different dangling chain configurations are compared. The studied materials are expected to find application areas ranging from antifouling to functional decorative coatings, and from marine to healthcare industries.

Many experimental studies have explored the molecular morphology of PU systems by using a variety of methods, such as scattering [18], thermo-mechanical [19], and scanning probe microscope [20]. Parallel to this, a large number of MD simulation studies have been conducted to provide supplemental information on the subject [21–27]. Also, there are several experimental techniques which can be used to detect the segregation of chains towards the interfacial layer, including water contact angle [28,29], AFM [30], X-ray photoelectron spectroscopy (XPS) [31,32], and quartz crystal microbalance (QCM) [33]. The majority of these methods cannot give a direct molecular-scale understanding of the segregation at the interface of polymer and a liquid material (mainly due to the ultra-high vacuum condition); therefore, the exact molecular behavior of materials at the interface cannot be fully captured by them. Thus, molecular simulation is an effective tool to combine with experimental surface techniques to investigate molecular morphology of polymer coatings at the interface with liquid materials.

In this work, we employ a dual mesoscopic (DPD [34–36]) and coarse-grained (CG) molecular dynamics (MD) simulation method (MARTINI model [37]) to investigate coating's interfacial properties and explore the capability of each method. Prior to this work, these methods have been separately used to explore polymer coatings' structure-property relationships. For instance, Kacar et al. employed DPD to study cross-linked epoxy coatings with an alternative parameterization, where the bead sizes are dictated by their experimental pure-liquid volumes [38]. Later, the material properties of the epoxy coatings were investigated by a multi-scale molecular simulations approach combining coarse-grained and all-atom molecular dynamics simulations via a reverse-mapping algorithm [23]. Iype et al. investigated the micro-phase separation of PU networks containing HPI dangling chains by means of the mesoscopic simulations [21]. They found out that there is a clear phase-separation of the dangling chains at the nanoscopic scale. Also, Ghermezcheshme et al. introduced a MARTINI-based method to build up cross-linked coatings with HPI dangling chains [39] and studied their interface with water [40], where they found that the interaction between the HPI dangling chains and water plays a significant role in the water dynamics at the interface. Note that Martini is capable of preserving near-atomic resolution and distinguishing hydrogen bond donor and acceptor groups; therefore, it is a reasonable model to be used for polyurethane systems at the interface with polar and apolar moieties (i.e., water and oil, respectively).

In the current work, we perform a dual approach simulation approach to, first, study the molecular morphology of smart PU coatings modified by HPI, HPB, and amphiphilic dangling chains, at water and oil interface and then, explore the capability of different simulation techniques with different resolutions in studying interfacial morphology of polymer coatings. To this end, we investigate the behavior of three different polycarbonate-based PU networks: 1) containing only HPI dangling chains, 2) composed of separate HPI and HPB dangling chains, and 3) containing amphiphilic dangling chains. All systems are considered as adaptive PU surfaces and their ability to adjust against different environmental conditions (i.e., HPI (water) and HPB (oil) interfaces) are evaluated. The structural and dynamic properties of the dangling chains regarding different interfaces are also discussed.

2. Materials and methods

2.1. Materials

In our simulations, poly(hexamethylene carbonate) macrodiol (PC) (M_w = 2000 g/mol), tris(isocyanatohexyl)biuret (HDI-BT), methoxy polyethylene glycol (mPEG) (M_w = 750 g/mol), 1-octadecanol (oDEC), and polyoxyethylene (20) stearyl ether, are used to construct the cross-linked polymer, and *n*-butyl acetate (nBAC) and ethyl methyl ketone (MEK) are used as the solvent molecules. PC and HDI-BT acts as the diol and cross-linker molecules, mPEG and oDEC chains are the hydrophilic (HPI) and hydrophobic (HPB) dangling chains, respectively, and polyoxyethylene (20) stearyl ether (Brij™ S20) is the amphiphilic dangling chain. Note that Brij™ S20 is composed of exactly similar size of mPEG and oDEC as used for HPI and HPB dangling chains. Water and octane molecules are used in modeling HPI and HPB interfaces. Therefore, we simulated three coating systems: *i*) PU network with HPI dangling chains (mPEG), *ii*) PU network with mixed dangling chains (mPEG and oDEC), and *iii*) PU network with amphiphilic dangling chain (Brij™ S20). The weight ratio of dangling chain to diol is kept 15 wt% for all systems. The system compositions are given in the Supplementary Information (SI) (see, Tables S1–S3).

2.2. Dissipative Particle Dynamics simulation method

DPD is an off-lattice simulation method that simulates the time evolution of coarse-grained entities referred as *beads*. DPD is initially developed by Hoogerbrugge and Koelman [41] as an improvement to lattice gas automata [42] to study complex fluids. Thereafter, Groot and Warren [36] mapped DPD method onto Flory-Huggins (FH) mean field theory [43] to compute the mesoscopic interactions, which made DPD method to be applicable to complex matter such as polymers, lipids, biopolymers, etc. [44].

The time evolution of the coarse-grained beads is solved by Newton's equations of motions. The total force acting on a particular bead $\mathbf{f}_i$ is sum of three forces, namely conservative force $\mathbf{F}_{ij}^C$, dissipative force $\mathbf{F}_{ij}^D$, and random force $\mathbf{F}_{ij}^R$. The end-structure in DPD is dictated by the conservative force. The chemical bonds are modeled by means of a harmonic force $\mathbf{F}_{ij}^H$ and is added to the total force: $\mathbf{f}_i = \sum_{i \neq j} \left(\mathbf{F}_{ij}^C + \mathbf{F}_{ij}^D + \mathbf{F}_{ij}^R + \mathbf{F}_{ij}^H \right)$. The conservative force dictates the structure in DPD, which is mainly characterized by the experimental FH parameters [43]. In our DPD simulations, we use an alternative DPD parameterization to compute the parameter a_{ij}, where the local volumes around beads are obtained as a function of their pure liquid densities. The representation of pure liquid densities is required in DPD to model the proper experimental bead sizes in the simulations [45]. The conservative pure repulsive interactions and the soft non-bonded potential in DPD do not represent the preferential attraction between particular molecular groups. This is the case in our simulations, where the HPI-HPI (i.e., HPI dangling chains and water), HPB-HPB (i.e., HPB dangling chains and oil) interactions characterize the structure. We model these selective interactions by incorporating a separate force term added to the total DPD force as a Morse type interaction in the form of $V_{Morse} = e_{HB}[e^{-2\sigma(r-r_0)} - 2e^{-\sigma(r-r_0)}]$, where

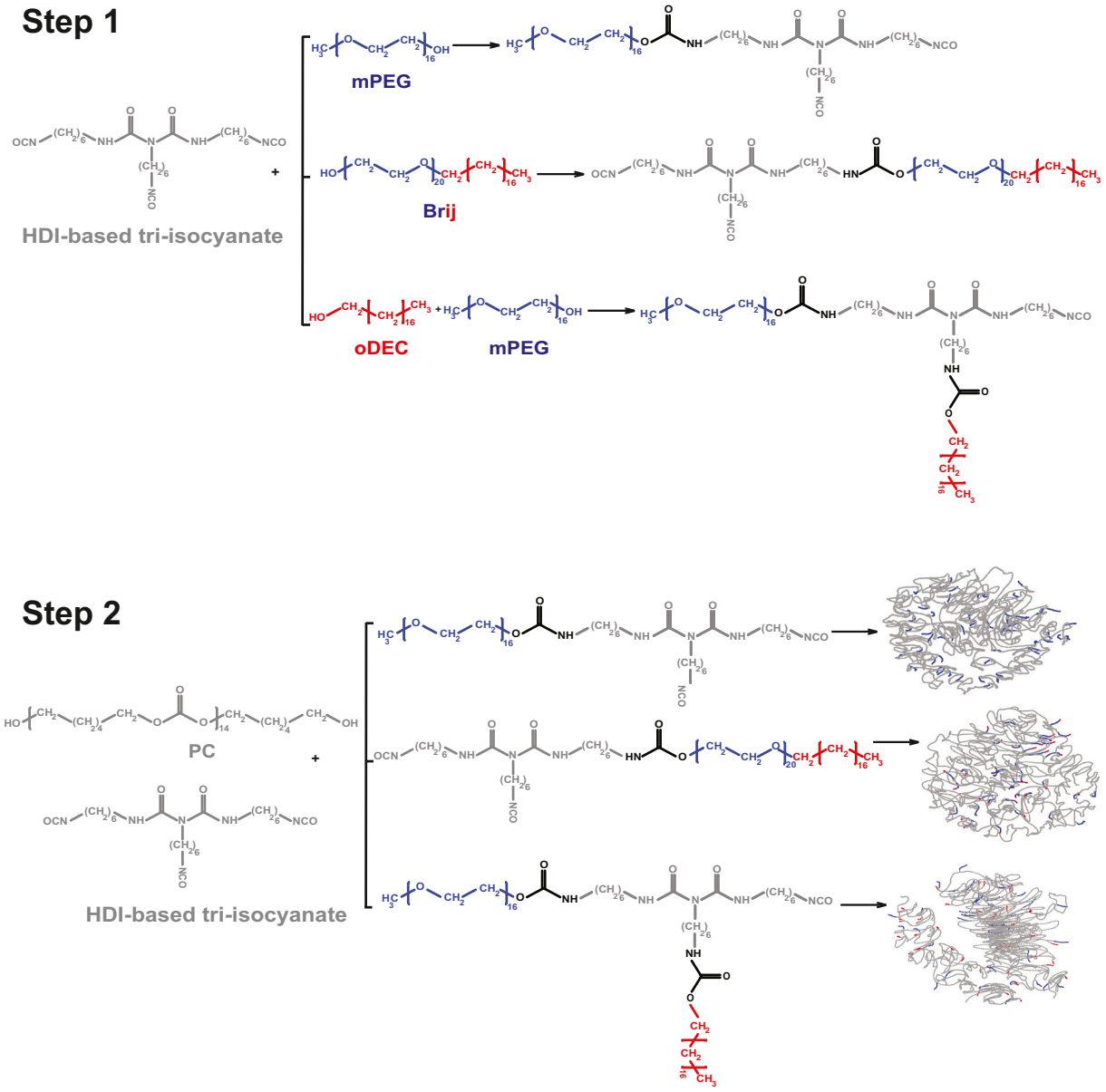

Scheme 1. Two-stage polymerization of PU coatings. The first step (step 1) results in dangling chains attached to the cross-linker (prepolymer) and in the second step (step 2), the final PU networks are made by introducing macrodiol (PC) and additional cross-linker.

$r < r_{DPD}$. In this relation, e_{HB} is the strength of the potential, σ is the curvature of the potential and r_0 is the equilibrium distance value. In our work, we adopt the parameters of the Morse potential as yielding similar strengths of HPI-HPI and HPB-HPB interactions and set as 7.96 k_BT and 5.0 k_BT, respectively. This procedure has been previously shown to model the physical properties of polyethylene glycol (PEG) [46–48], three-dimensional tetrahedral structure of water as computed from the three-body angular distributions [49], and in modeling ibuprofen encapsulation in poloxamer micelles with a good prediction of the experimental structural and drug encapsulation properties [50]. The coarse-graining procedure is done based on partitioning the chemical functional groups of the systems as mentioned above. The schematic representations and bead definitions are given in Fig. S1 of the SI with the technical details of the DPD method.

2.3. MARTINI simulation method

The MARTINI method, presented by Marrink et al., is one of the effective models for coarse-grained simulation of Macromolecules [37,51]. It was developed initially for the simulation of lipids and biomolecules, and later applied to other molecules, such as proteins [52], carbohydrates [53], DNA [54], solvents [55], polymers [56,57], coatings [58–60] and amphiphilic surfactants [61]. In the MARTINI approach, coarse-graining of atoms into beads is no longer a purely defined process, and the number of heavy atoms assigned to a bead can be 2, 3, or 4. There are four types of interaction sites for MARTINI beads: polar (P), nonpolar (N), apolar (C), and charged (Q), each of which is further divided into subtypes based on the polarity and hydrogen bonding ability. The ability of the MARTINI force field to distinguish between beads with hydrogen bond donor or acceptor capacity makes this a suitable force field for simulating polymeric systems, particularly polyurethane. Fig. S3 illustrates the mapping and standard MARTINI bead type for each bead.

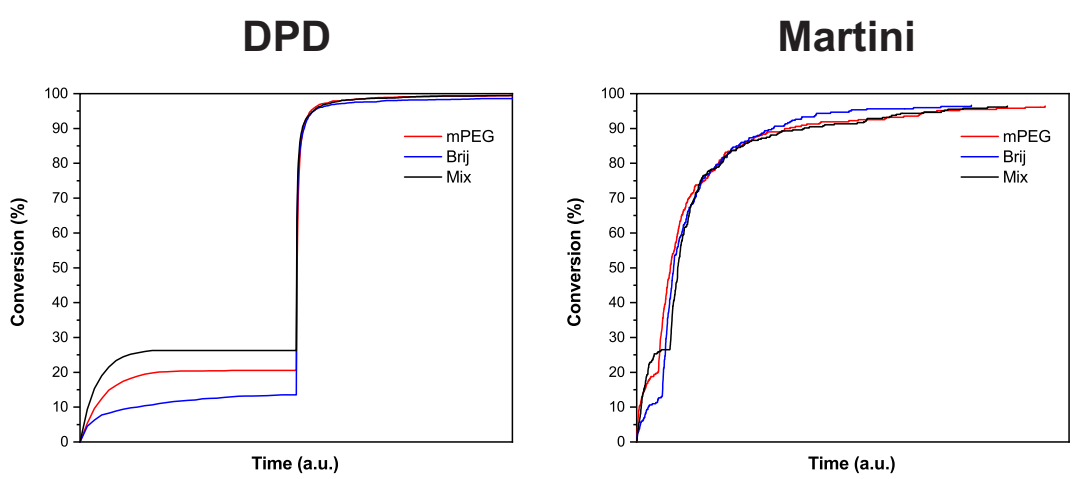

Fig. 1. Cross-link conversion values in percentage for different cross-linked systems as a result of two-step cross-link formation.

2.4. DPD simulation details

Initially, we create the cross-linked bulk PU structures for each system. The PU network were composed of a total number of 128,625 beads in simulation boxes corresponding to a dimensionless number density of 3 and box size of $35 \times 35 \times 35\ r_{DPD}^3$. A generalized flowchart in Fig. S2 in the SI summarizes the DPD simulation steps of all three simulated systems.

To model the cross-link formation, a previously employed procedure that creates a covalent bond if the distance between two cross-linking beads is below a defined cut-off distance is used. This procedure has been observed to create cross-linked structures of bulk epoxy [38], epoxy near interfaces [24] and PEG hydrogels [22] in line with the experimental findings. The cut-off distance is selected as 0.4 r_{DPD}. The resulting new bead types are incorporated in the simulations and their interactions are updated correspondingly.

Afterwards, these PU systems are simulated as they interact with different interfaces. The created bulk PU systems are combined with water and oil layers. These 5 nm thick layers are modeled as two layers above and below the PU by expanding the box. The dimensionless bead number density of these layers corresponds to 3. Water molecules are coarse-grained by setting one water molecule as one DPD bead. The experimental solubility parameters as explained before are used to compute the DPD interactions of the HPB octane molecule (C_8H_{18}). While modeling the polyurethane/oil interface, and the octane molecule is represented in the system as a single bead. The aim here is to imitate a HPB surface by means of creating an oil surface. The beads forming the different surfaces are fixed at their original coordinates with a harmonic potential with the constant value of 100 k_BT/r_{DPD}^2. Fixing the beads at their initially created coordinates is done in order to prevent the penetration of these beads into the polymer. This approach is previously shown to represent the experimental interfacial behavior of liquid mixtures on the air interface by DPD simulations [48]. An interfacial thickness of around 10 nm is taken as to compute the DPD interactions of water/oil surfaces. The DPD simulations are carried out at 0.02 t_{DPD} time step and with a total number of additional 500,000 steps restarted after the bulk system is finished at the *NVT* conditions. LAMMPS molecular dynamics package is used in all of the DPD simulations [62].

2.5. MARTINI simulation details

The GROMACS simulation package is used to run CG MD simulations using MARTINI method. The interaction parameters (σ and ε) for the non-bonded interaction are based on standard MARTINI bead types. For all materials, the bonded interaction parameters are shown in Tables S16 and S17. The validity of the bonded and non-bonded interactions has been proven in our previous papers [39,60]. Also, we used the same parameters that Grunewald et al. presented for non-bonded interactions of HPI beads with water [63].

In order to create 3D polymeric networks, we use our recently developed CG MD method [39]. Similar conditions and sequence are used as in the DPD method to form the polyurethane networks. In order to equilibrate the generated networks, we run a *NPT* simulation for 50 ns at 25 °C and 1 bar using a 10 fs time step. To control the temperature and pressure, respectively, V-rescale and Berendsen algorithms are used. In order to investigate the interaction between polymer networks and oil or water, a slab of water or oil is placed on top of the networks. With a 10-fs time step, an *NVT* equilibration is performed over 50 ns. To study the switchability of the polymeric network, the water slab was removed from the top of the network. A slab of oil was then placed on top of the polymeric network. After running an *NVT* simulation, the oil slab was removed and a water slab was placed on the network. This was followed by another *NVT* simulation.

3. Results and discussion

3.1. Building the polymer network

Forming the bulk structures for the PU network is achieved by a two-stage polymerization (see, Scheme 1). It is shown that a two-stage reaction prevents the possibility of functional dangling chains fail to bind with the cross-linker [39]. As shown in scheme 1, the first stage of reaction is between the cross-linker (HDI-BT) and different dangling chains (mPEG (HPI), 1-octadecanol (HPB), or Brij™ S20 (amphiphilic)). The second step consists of the reaction between the prepolymer and the polyol, as shown.

The cross-linking conversion value is obtained by dividing the number of reacted beads by its initial number. The time evolution behavior of the cross-linking conversion for both simulation methods is depicted in Fig. 1. It is noticed that the cross-linking conversion profiles continue to increase in time in a decreasing rate, which seem to stabilize at the end. There is no scaling of time-steps done for DPD and MARTINI simulations; therefore, different simulation times regarding step 1 and step 2 can be noticed in Fig. 1. As shown, both methods lead to a rather high final conversion (above 93 %), which indicates that fully cross-linked PU networks have been obtained from both methods. Note that DPD potentials are rather softer as compared to MARTINI ones; therefore, beads could find each other within the reaction cutoff easier and higher reaction conversions are possible in DPD simulations.

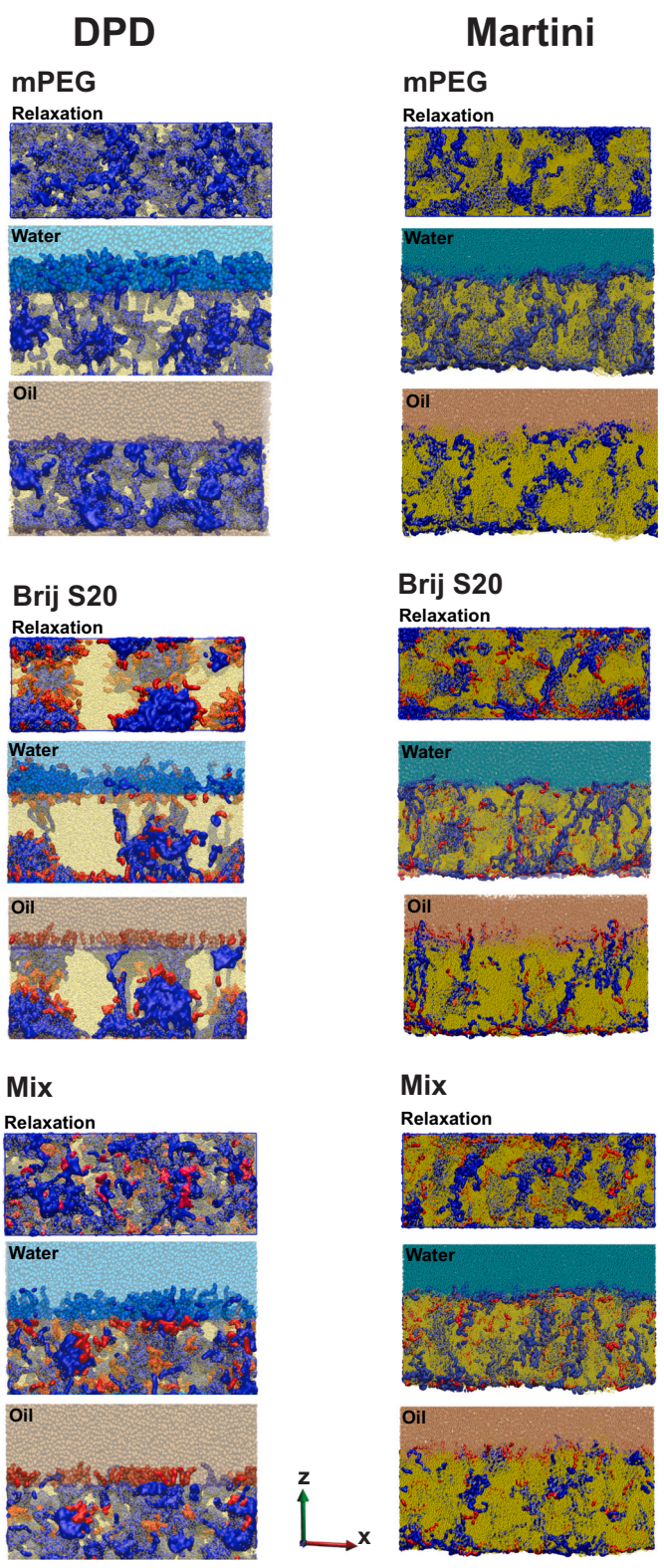

Fig. 2. Simulation snapshots of 15 % mPEG, Brij™ S20 and Mix systems for layer-free, water and oil layer simulations. Left and right columns depict DPD and MARTINI simulation results. Red and blue color show HPB and HPI dangling chains, respectively. Yellow color is used to represent the rest of the coating's structure. (For interpretation of the references to color in this figure legend, the reader is referred to the web version of this article.)

3.2. Interface behavior of PU at water and oil surfaces

To study the interface structure as influenced by different interfacial characters, we simulate two different interfaces interacting with the bulk PU namely, water and oil layers. The cross-linked PU structures that are obtained in the previous section are taken as the polymer layers. Later, in DPD simulations, the PU structure is positioned in the middle of the box and water and oil layers are positioned on top and bottom of the coatings with a 5-nm-thick layer on each side of the PU in z-dimension. For MARTINI modeling, 5-nm-thick water and oil layers were positioned only on top of the polymer layer. For all analysis, we only considered the interface of the polymer and top water/oil layer to be consistent in comparing DPD and MARTINI results.

In Fig. 2, the interfacial structures of mPEG, Brij™ S20 and Mix systems are shown as influenced by the presence of different surfaces. In the systems that contain only mPEG dangling chains, both DPD and MARTINI simulations yield similar results such that the HPI groups are penetrated to the water interface. The structure as observed from the snapshots is also indicating some level of clustering of HPI groups inside the bulk structure (with and without the presence of water layer). In oil, as expected from a PU containing only HPI dangling chains, there is no penetration of mPEG (dangling) chains inside the oil layer. Only a very small portion of (HPB) groups of PC is noticed to be present inside the oil layer in the DPD simulations.

The switchability of the PU containing mixture of HPI/HPB chains and amphiphilic Brij™ S20 chains is more clearly noticed in these systems as influenced by different types of interfaces. Both DPD and MARTINI simulations exhibit surface penetration of HPI groups at water interfaces and vice versa for Brij™ S20 and Mix systems. The surface enrichment of the HPI and HPB groups in their corresponding surfaces are noticed to be higher in DPD simulations as compared to the MARTINI simulations. The effect of the soft non-bonded potential nature of the DPD method might result in this behavior. Clustering of HPI groups is noted again in both DPD and MARTINI simulations, being higher in the former method. This is more noticeable in Brij™ S20 system compared to the Mix system. The surface-free snapshots (indicated as *Relaxation*) depict this clustering as well. In general, the surface-free simulations indicate similar level of structures as in the case of water and oil layers.

A quantitative interface characterization is also done by computing the number of HPI or HPB beads that migrate to the water or oil layer over simulation time by measuring the percentage of HPI and HPB beads that are present in the water or oil layer. To calculate this value, the density profiles of dangling chains at various times of simulations are analyzed. Using the trapezoidal method, the integral of the density profile graph (at $z >$ interfacial region) is calculated at each time point. By multiplying the integral values by the x and y dimensions of the simulation boxes, we can determine how many beads are present in the water or oil layer. By dividing this value by the total beads of HPI or HPB of dangling chains, the percentage of HPI or HPB in water/oil layer is determined. By this way, we can monitor the dynamics of the surface enrichment of the chains and intrinsic surface migration of the systems at different interfaces in time. It should be noted that the time-dependent density profile and dangling chain orientation towards the water/oil interface suggests that a (quasi) equilibrium state has been reached after 25 ns, as indicated in Fig. 3 (formation of plateau) and in more detail for all Martini cases in Figs. S4 and S5 in SI.

In Fig. 3, the surface integrals indicate a clear migration of the chains towards the interfaces for both DPD and MARTINI simulations. A clear difference is noticed in between the water and oil surfaces. For mPEG in water, the accumulation of HPI chains is more pronounced as compared to the same system in oil. The HPB groups in the amphiphilic Brij™ S20 chain exhibit rather strong immediate segregation upon interacting with oil interface in MARTINI simulations. However, DPD predicts that the HPI groups in water have the fastest segregation rate in this system. This behavior is followed by HPB groups in oil, as expected. The HPB groups

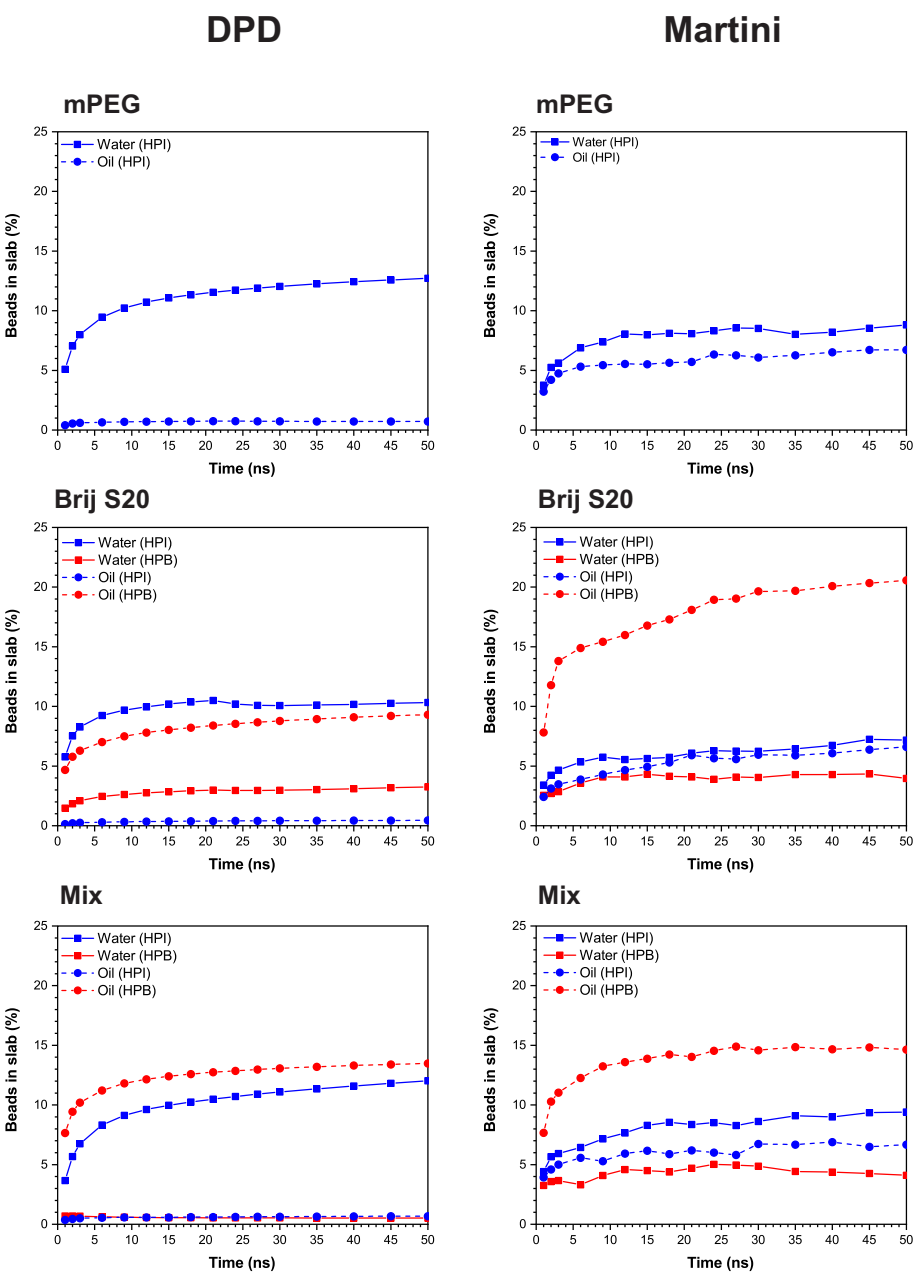

Fig. 3. Percentage of HPI and HPB beads present in water or oil layer plotted as a function of simulated time for DPD and MARTINI simulations. Blue and red colors depict HPI and HPB groups, respectively. Filled circles and squares show oil and water interfaces consecutively. (For interpretation of the references to color in this figure legend, the reader is referred to the web version of this article.)

in water and HPI groups in oil are still dragged towards these interfaces since they are attached to the rest of the chains although they have unfavorable properties. In the Mix system, both methods predict that the surface segregation of HPB groups in oil as the fastest. Moreover, the diminishing percentage of the HPB beads in water layer indicates that the HPB dangling chains in the Mix system prefers to move inside the bulk PU. In all, the surface segregation of dangling chains is predicted in a reasonable agreement between MARTINI and DPD simulations apart from the amphiphilic system, where the fastest segregation rate is noticed for HPI in water by DPD and for HPB in oil by MARTINI. Overall, the affinities of the functional groups with respect to the similar surfaces are captured as expected from chemical intuition. Using similar systems as those studied in this paper, experimental work has demonstrated that hydrophilic chains segregate towards the water layer. X-ray photoelectron spectroscopy and water contact angle analyses showed that samples with higher mPEG chains are more hydrophilic, indicating the presence of mPEG chains at the water-polymer interface [9].

3.3. *Structural properties of dangling chains as influenced by interfaces*

We investigated the effect of different interfaces on the dangling chain conformation by computing the end-to-end distance R_{ee} of dangling chains, as shown in Fig. 4. Temporal evolution of the chain length gives a quantitative information on how the chain structures on average are affected by the penetration towards the interfaces. In water interface, mPEG system yields more elongated HPI chains compared to oil interface. If the Brij™ S20 system is considered, the R_{ee} values at water and oil interfaces are almost the same as predicted from the DPD simulations. Although, there is a qualitative agreement in between, there is a higher level of difference between R_{ee} of amphiphilic dangling

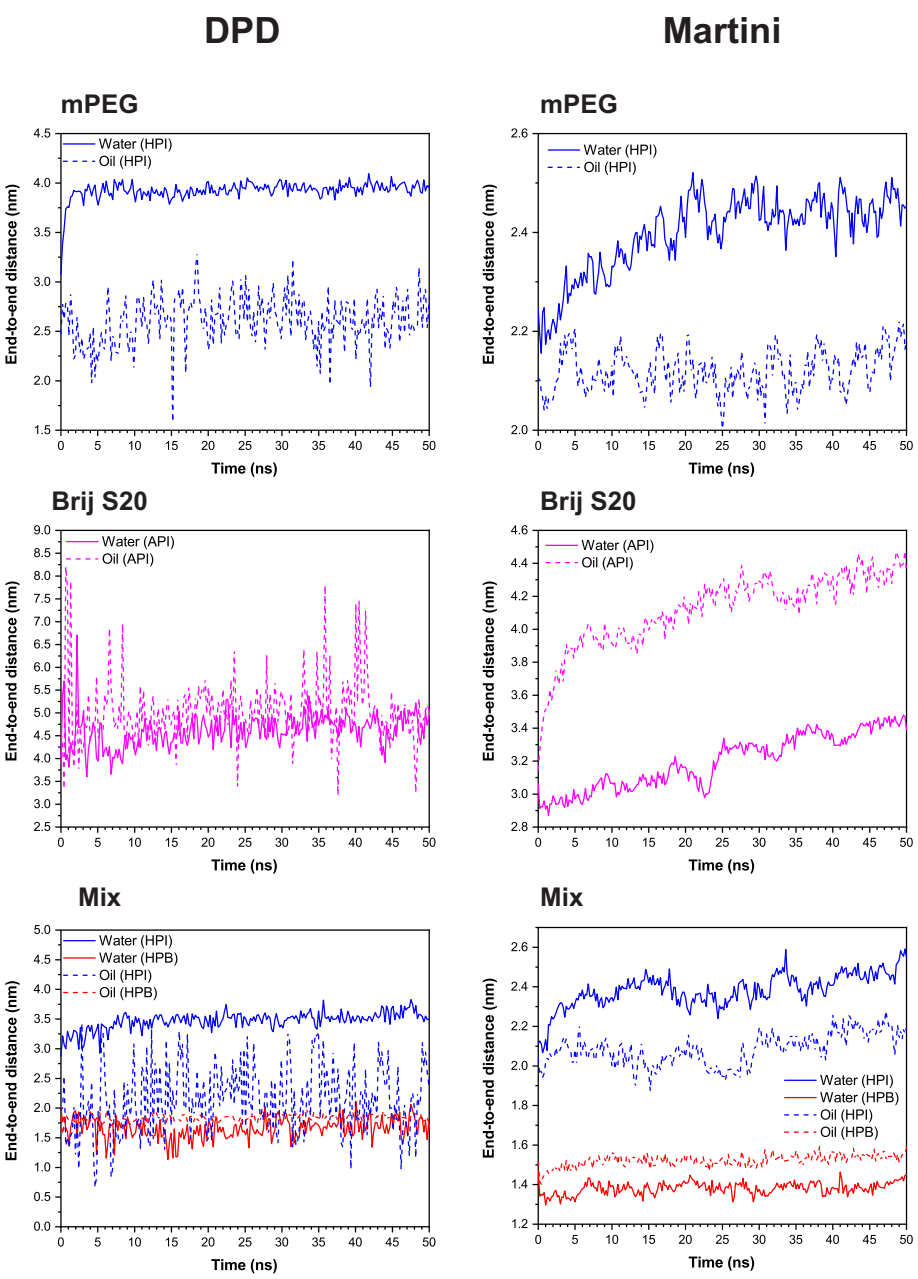

Fig. 4. End-to-end R_{ee} distance values as computed for water and oil interfaces for the HPI and HPB interfaces and plotted as a function of time.

chains at water and oil interfaces predicted by MARTINI and DPD simulations for the Brij™ S20 system. For the Mix system, the HPB chains form rather compact structures at all interfaces in contrast to HPI chains. The HPI chains in water adopt relatively more extended conformations, which is completely opposite in oil interface. In general, the difference in the R_{ee} values of the HPI chains is much higher as compared to the HPB chains in water and oil interfaces, respectively. The effect of water on the HPI chains is more dominant as compared to the effect of oil interface on HPB chains. This can be explained by the fact that the length of HPI chains (i.e., number of repeating units) is greater than the HPB ones, yielding higher level of interaction with the water at interface. In general, the simulation times are noticed to be long enough to fully equilibrate the systems since the curves are almost flattened at the end of the simulations for both DPD and MARTINI. A fast equilibration of chains is noted for the Mix system by both simulation methods as observed from the swift equilibration of the R_{ee} curves. For the rest of the systems, the structures equilibrate faster in DPD (most-likely) due to the soft non-bonded potential of the DPD method. In MARTINI, systems equilibrate slower as a result of the presence of higher level of complexity (precision) in interactions. Overall, there is a qualitative agreement between the DPD and MARTINI simulations. The absolute R_{ee} values as predicted by both systems might be different due to the different level of coarse-graining and the resulting physical length-scale of DPD. Nevertheless, the sequence of the predicted behavior of HPI and HPB chains under different interfaces for the studied systems are the same, which renders a qualitative consistency of the two methods. This means that the intrinsic character of chains is captured via molecular simulations performed with different techniques with different resolutions.

The local structures of dangling chains are studied by computing the radial distribution functions (RDF) in our work. We compute the RDF profiles for the HPI-HPI, HPI-HPB and HPB-HPB interactions at different interfaces for different systems simulated by MARTINI and DPD methods. The HPI-HPI interactions in the bulk system in Fig. 5 show

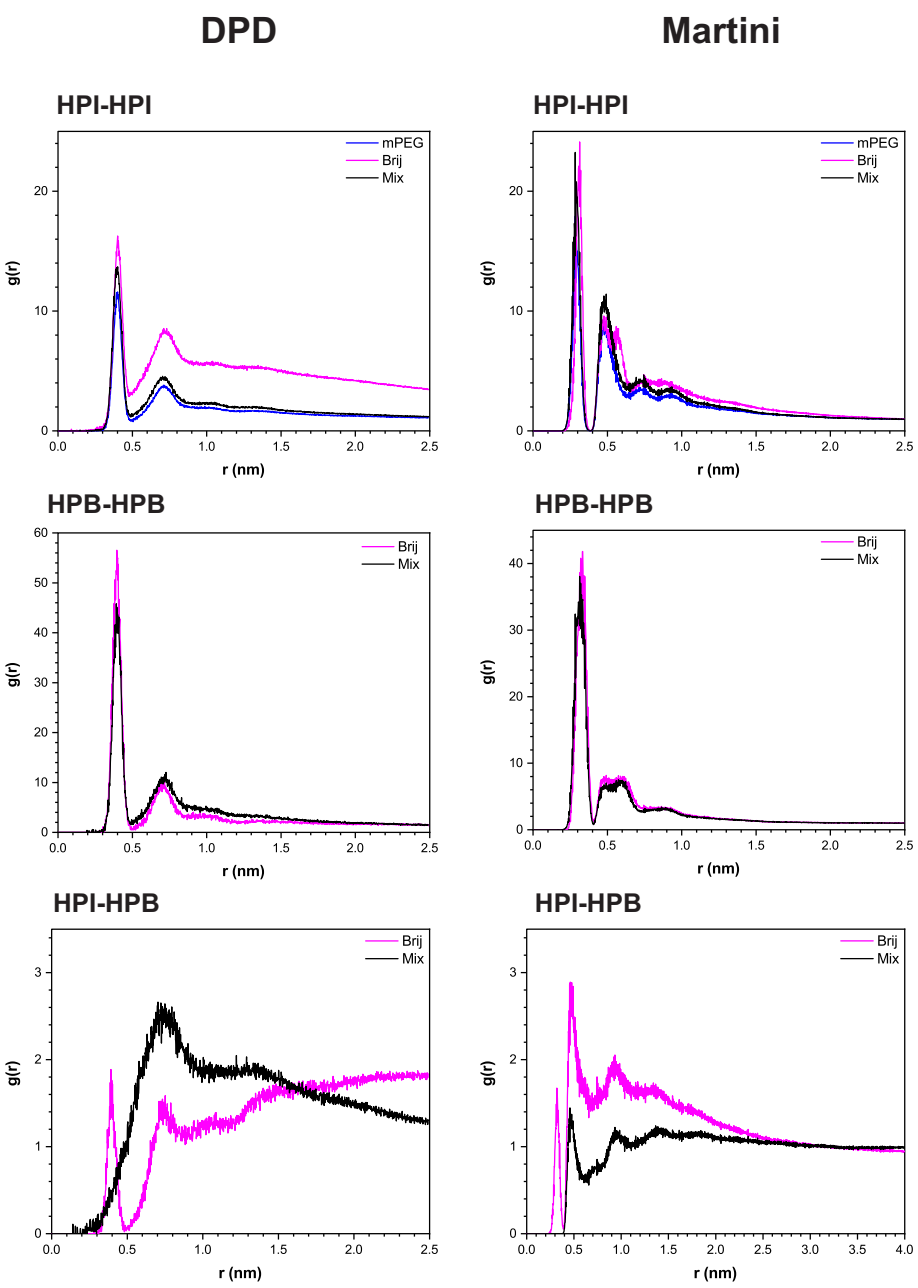

Fig. 5. Radial distribution functions for HPI-HPI, HPB-HPB, and HPI-HPB groups for the simulated Mix (black color), mPEG (blue color), and Brij™ S20 (pink color) systems without the presence of an interface (bulk simulation). (For interpretation of the references to color in this figure legend, the reader is referred to the web version of this article.)

rather different behavior for the Brij™ S20 system as compared to the Mix and mPEG systems in the DPD simulations, whereas MARTINI simulations predict similar structures, as expected. The difference between Brij™ S20 and mPEG and Mix systems can be attributed to the difference in the FH parameters of HPI-HPI interactions (see, Tables S5, S9 and S13). There is a higher repulsion between the HPI groups in Mix and mPEG systems as compared to the Brij™ S20 system. The HPI-HPI interactions are quite similar to each other with a high first peak for the first neighboring shell for Brij™ S20 and Mix simulations. The HPI-HPI interactions show somewhat different behavior for the Mix system in DPD and MARTINI simulations. Mixing of HPI and HPB beads are noticed for the Mix system, however, a rather small level of separation is clear from the DPD simulations with a farther peak location. Again, the DPD parameterization as based on the FH parameters affects the structure. High repulsion between HPI-HPI groups in the Mix system compared to the Brij™ S20 system is noted as the main reason for the observed difference.

Upon presence of water interface as shown in Fig. 6, the structure of the HPI groups are quite similar to the bulk system except a more coordinated first neighboring shell for DPD and MARTINI simulations. This indicates that the HPI groups are closer to each other in the water interface. Moreover, the discrepancy between the DPD and the MARTINI methods lessens. The HPB-HPB interactions also show a significant degree of attraction between the HPB groups. The influence of water as compared to the bulk system is more clearly noticed for the HPI-HPB interactions with an increased level of contact in Mix and Brij™ S20 systems. MARTINI simulations show a closer neighboring of HPI and HPB contacts in the presence of water as compared to the bulk system. The two simulation methods deviate with respect to the HPI-HPB interactions. The reason might be associated with the FH parameters of

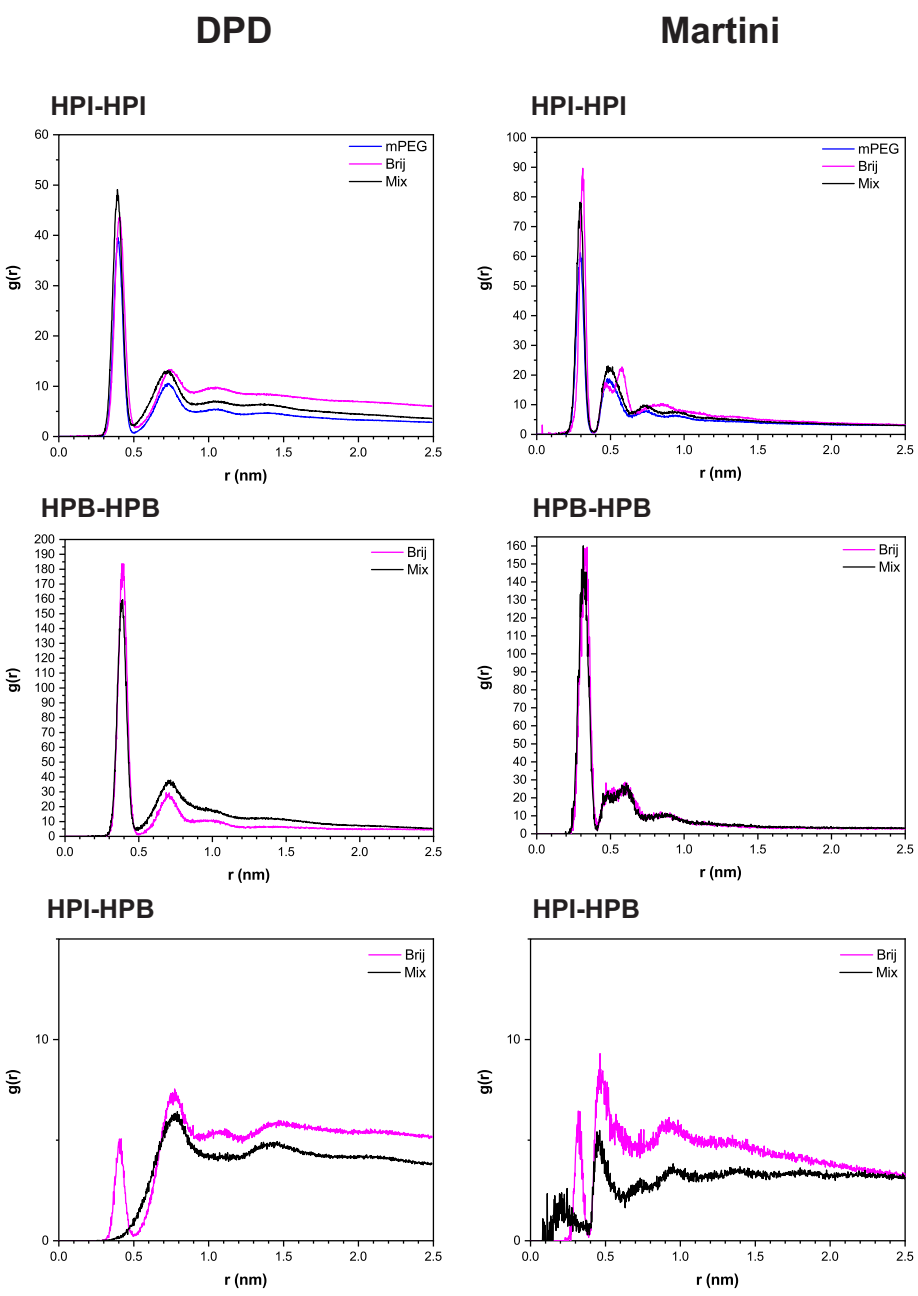

Fig. 6. Radial distribution functions for HPI-HPI, HPB-HPB, and HPI-HPB groups for the simulated Mix, mPEG, and Brij™ S20 systems interacting with water interface.

HPI-HPB beads (Tables S7 and S15 in the SI) dictating the DPD results, which lead to less repulsive interactions in the Brij™ S20 system compared to the Mix system. In MARTINI simulations, HPI-HPB interactions at very close bead separations are noticed for the Mix system in contrast to the repulsive FH interactions.

In Fig. 7, all the systems are exposed to oil interface and the corresponding structures are plotted. There is a significant difference as compared to systems at bulk and water interface for the DPD simulations. The presence of oil interface affects the HPI chains in bulk so that the HPI beads are pushed together as noticed from the non-zero RDF values at small separations. This is true for both DPD and MARTINI methods, where is more dominant for the Brij™ S20 system. The HPB-HPB interactions of the MARTINI and DPD models are quite similar to the water interface. However, there is a very high concentration of HPB beads that are at very small separations from each other for the DPD simulations in the Mix system. This situation is not noticed in the Brij™ S20 one. A possible explanation to the overlapping beads can be made when the DPD interactions of individual beads forming the HPB chains are analyzed (Table S6 in the SI). The self-repulsion a_{ii} value of the end group of the HPB molecule (D bead in DPD method) is very small indicating a very small-sized bead (see also, Fig. S1 in the SI). Therefore, a very high repulsion between the D bead and the oil might lead to the overlapping D beads. A similar case is noted between the HPI-HPB interactions in both DPD and MARTINI simulations, where non-zero RDF values are noticed at close bead separations for the Mix system. The possible overlapping of small beads, namely the end-groups of HPI and HPB beads on top of each other in the presence of oil surface might induce this resulting structure.

The structural interactions of the dangling chains and their difference are evaluated in Fig. 8 by computing the RDFs of HPI and HPB chains at water and oil interfaces. It is clearly noticed that the structure of HPI chains in water and HPB chains in oil and vice versa behaves quite

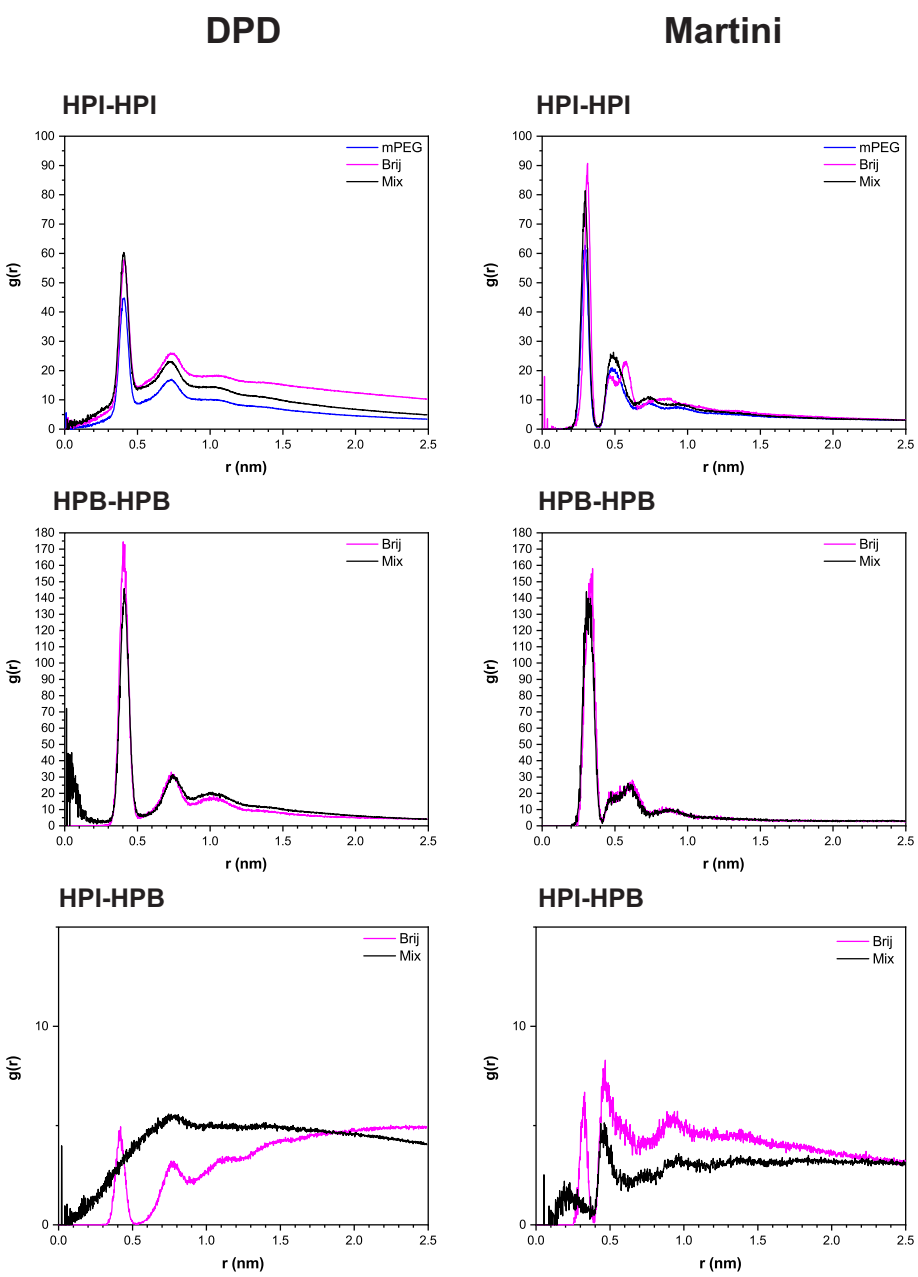

Fig. 7. Radial distribution functions for HPI-HPI, HPB-HPB, and HPI-HPB groups for the simulated Mix, mPEG, and Brij™ S20 systems interacting with oil interface.

similar as deduced from MARTINI simulations with a minor difference for different systems. This is also true for the DPD simulations. However, a higher level of attraction is noticed for the HPI-Water interactions of the Brij™ S20 system as compared to the Mix and mPEG systems. The repulsion between the HPI groups and water in Brij™ S20 system is less compared to the Mix and mPEG systems (see, FH parameters in Tables S7, S11 and S15). The less repulsion in between HPI and water leads to more elongated chains in the DPD simulations as observed from the higher R_{ee} values of Brij™ S20 system in Fig. 4. These might explain the significant degree of interaction of HPI with water as a result of the larger contact area of the chains with water. Similarly, smaller FH parameters of hydrophobic groups and oil leads to a more extended HPB chain for the Brij™ S20 system as compared to the Mix system (see, Fig. 4). The HPB groups and their oil interactions are quite comparable for the two simulation methods.

The RDFs are computed irrespective of the dangling chain location for all systems. Therefore, the computed RDFs are affected from the bulk concentration of dangling chains even if there is a high surface enrichment at a particular interface. For example, the less concentration of HPI groups of Brij™ S20 system in bulk region at the water interface as compared to the Mix and mPEG systems (see, Fig. 2) might be another cause of the higher peak of this system in Fig. 8. Nevertheless, there is a reasonable agreement between DPD and MARTINI simulation results apart from the discrepancies mentioned above.

3.4. Adaptive surface behavior and switchability of the PU surfaces

So far, the molecular morphology of the dangling chains are discussed as they are simulated in a single interface. In this section, we further simulate these systems as the interface structure is changed from one to another in order to study the adaptability of the PU coatings. To that purpose, the structures that are simulated while interacting with a particular surface are rerun at a new surface. In DPD simulations, the corresponding set of parameters are updated for the new surface.

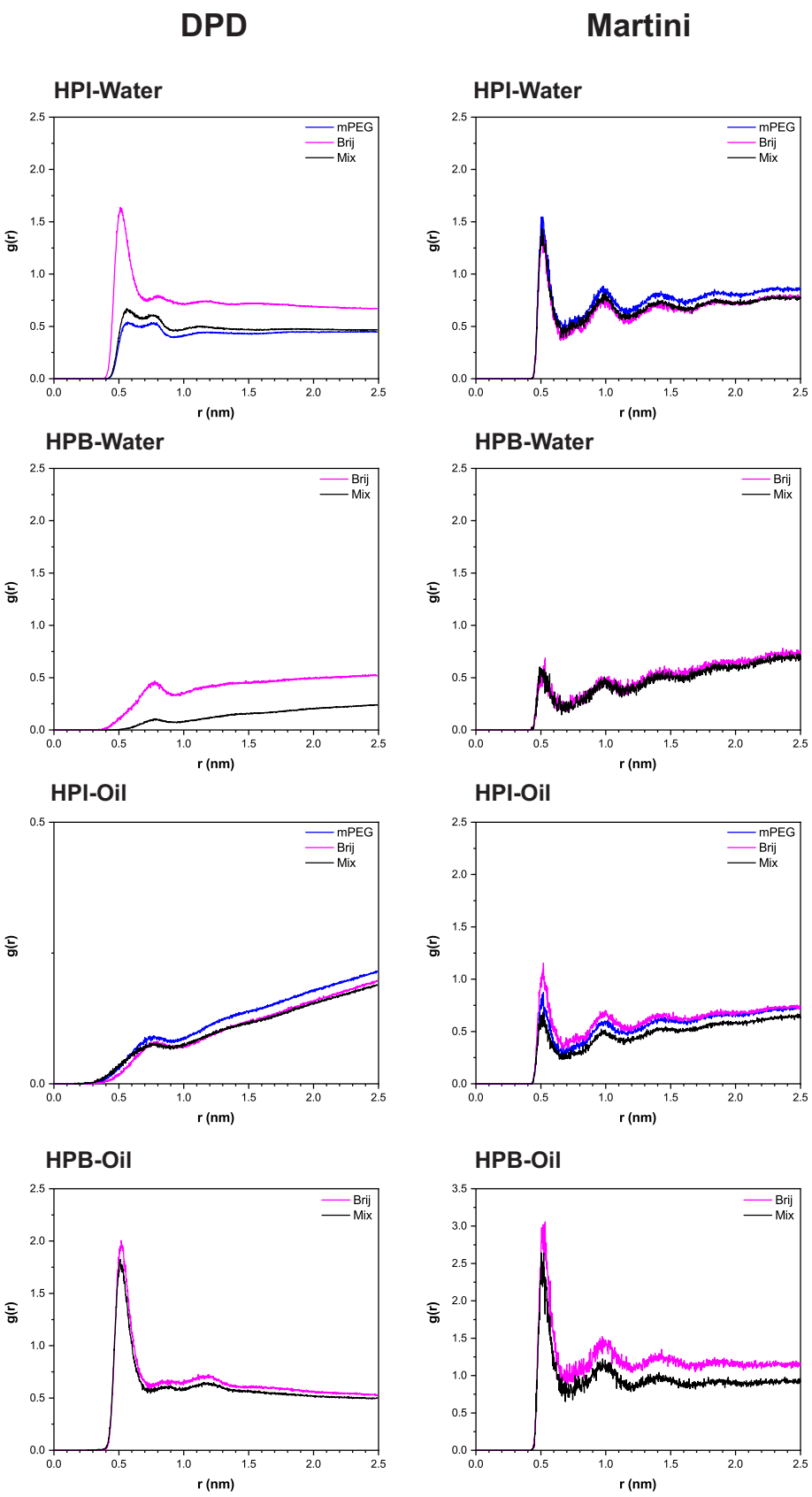

Fig. 8. Radial distribution functions for HPI-Water, HPB-Water, HPI-Oil and HPI-Oil molecules for the simulated Mix, mPEG, and Brij™ S20 systems.

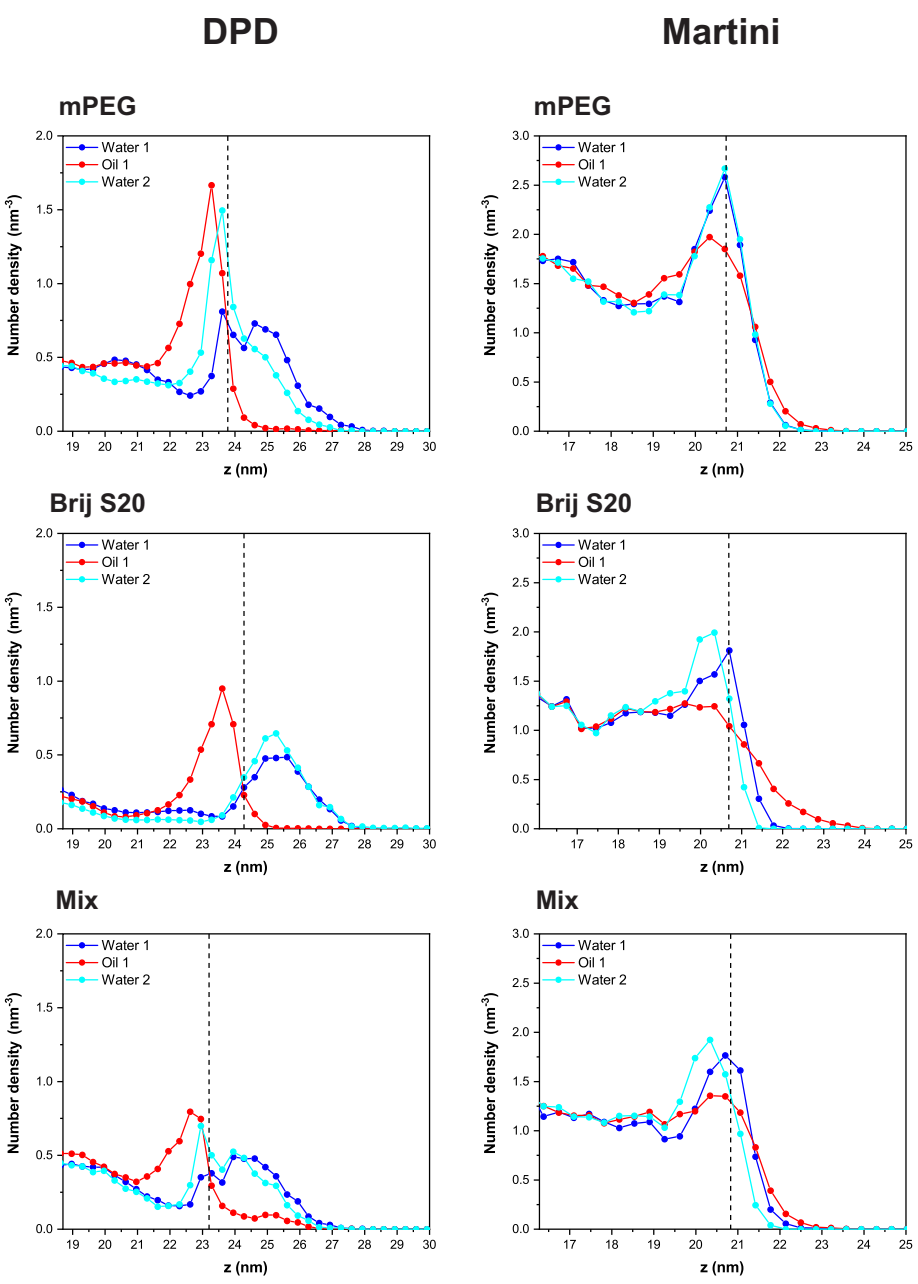

Fig. 9. Density profiles of the DPD and MARTINI simulations as computed for the hydrophilic portion of the dangling chains in the sequence of initially water (water 1-blue color), oil (oil 1-red color) and finally water (water 2-cyan color) interfaces for mPEG, Brij™ S20 and Mix systems. The graphs are displayed from the middle of the polymer layer to the end of the slab. The location of the interfaces is shown with dashed line. (For interpretation of the references to color in this figure legend, the reader is referred to the web version of this article.)

Thereby, we can comment on the adaptability and switchability of the PU coatings as the nature of environment is changed from HPI to HPB and vice versa.

Firstly, we plot the density profiles for the HPI chains as the coatings are interacting with water-oil-water cycles in Fig. 9. In other words, the PU coating is initially interacting with water. Then, the surface beads are changed to oil. And as a final step the oil surface is switched back to water. The simulations are run long enough to maintain the equilibrium structures as done in the previous steps and the corresponding density profile is computed.

The HPI groups of dangling chains are observed to adopt a switchable behavior as interacting with the mentioned interface cycles. mPEG chains initially migrate inside the water interface. Later, oil surface drives these chains back towards the bulk polymer and finally, the chains move again towards water surface as the surface is changed from oil to water. This comment is made such that the peak location of the oil interface decreases in DPD and lessens in MARTINI methods. The MARTINI simulations dictate that the HPI group concentrations are almost the same in initial and final water layer. However, the density profiles of the HPI portion of the dangling chains in the initial and final water layer are somewhat different in DPD simulations for the mPEG system. This discrepancy can be associated with the positioning of the PU in DPD modeling scheme. In DPD, we position the PU layer in the middle of the interfaces, therefore yielding two interfaces in a particular periodic image. In Figs. 9 and 10, we show only the top interface. Nevertheless, we still observe a preferential segregation of hydrophilic portion of the dangling chains in the final water interface for DPD simulations. In Brij™ S20 and Mix systems, the density profiles of the initial and final water layers are quite similar for the DPD simulations. Moreover, we observe a significant concentration of HPI dangling chains inside all surfaces in MARTINI simulations, whereas in DPD the HPI chain concentration is quite low in oil for all systems. The only exception is the Mix system, where there is somewhat limited concentration of HPI chains inside oil in DPD. This may be attributed to the HPB groups that are attached at very close locations to the HPI groups during cross-linking. In other words, the HPB interactions may drag HPI groups

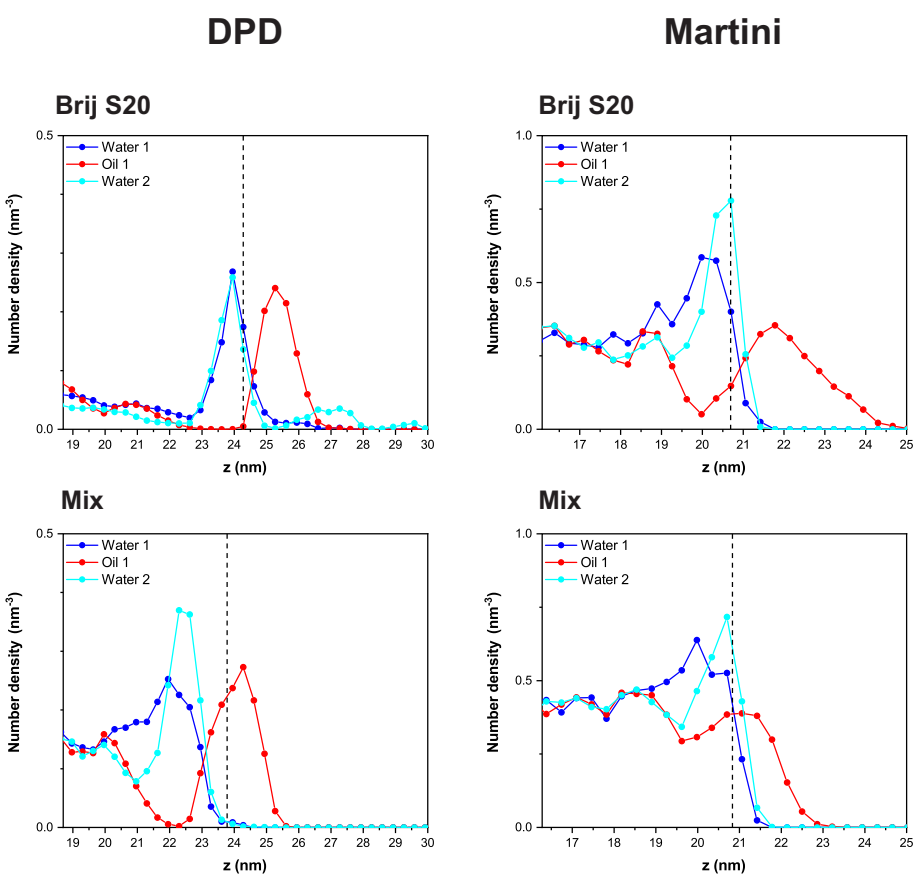

Fig. 10. Density profiles of the DPD and MARTINI simulations as computed for the hydrophobic portion of the dangling chains in the sequence of initially water (water 1-blue color), oil (oil 1-red color) and finally water (water 2-cyan color) interfaces for mPEG, Brij™ S20 and Mix systems. The graphs are displayed from the middle of the polymer layer to the end of the slab. The location of the interfaces is shown with dashed line. (For interpretation of the references to color in this figure legend, the reader is referred to the web version of this article.)

towards oil layer. Again, a limited concentration of HPI groups in oil layer is noticed in MARTINI simulations as well.

In Fig. 10, the behavior of HPB groups of the dangling chains is shown under switchable surfaces. In general, the Brij™ S20 and Mix systems exhibit penetration of HPB groups towards oil layer, whereas in water HPB groups are mainly present inside the bulk PU. This is true for both DPD and MARTINI simulations. The HPB groups in water are mainly at the water interface for all systems except the Mix as system simulated by DPD. The excessive repulsive strength between the HPB groups and the water layer pushes these groups inside the bulk polymer. However, there is a small portion of HPB groups trapped inside the water layer in the second cycle for the Brij™ S20 system due to the amphiphilic nature of the molecule. The penetration of HPB groups to the oil layer in the prior simulation introduces a bias to the structure, so that very little concentration of HPB groups remains inside the water layer. In all, the surface HPB dangling chains adopt a switchable property, where these groups are mainly present at locations close to interfaces.

4. Conclusions

In this work, we employ molecular simulation tools to understand the intrinsic structure and dynamics associated with particular PU coatings with (HPI, HPB, and amphiphilic) dangling chains at their interface with water and oil. The simulations are performed at two different resolutions, where a different level of coarse-graining is attained. The reason for using two different simulations is neither to compare nor to verify these methods. Instead, we are motivated to make use of the different levels of resolution to draw a more general conclusion that would yield results of the studied system irrespective of the used simulation method.

The dangling chains are HPI and HPB in nature, where pure HPI, a combination of HPI and HPB, and amphiphilic chains are simulated. Initially, we observe that the created cross-linked PU coatings achieve a high degree of cross-linking conversion during the formation of their bulk structures. In the bulk structures, somewhat clustering of HPI chains is noticed. This is more dominant in DPD simulations due to the soft and purely repulsive nature of the non-bonded potentials. Later, these bulk structures are exposed to the water and oil interfaces as to mimic the HPI and HPB surfaces in order to study the structure and surface segregation of the various dangling chains. The structure is mainly characterized by computing the end-to-end R_{ee} distances as a function of time and static radial distribution functions (RDF) for the equilibrated structures. The R_{ee} reveal that the HPI chains in water are rather in extended form compared to their conformation at the oil interfaces, whereas the amphiphilic chains rather adopt a more compact conformation in water as compared to the oil. The R_{ee} results are observed to qualitatively agree between DPD and MARTINI. Later, by computing the RDF plots, we observe that the HPI chains prefer to be near water, while HPB chains prefer to be mainly near oil. Although, there is a discrepancy between DPD and MARTINI RDF results, which is more dominant in HPI-HPB interactions in Mix and Brij™ systems, the intrinsic interactions of dangling chains under different surfaces are captured to a great extent. In order to study the segregation dynamics the presence of HPI and HPB beads that segregate into the water or oil layer is computed during simulation. Both simulations predict the fast dynamics of hydrophilic and hydrophobic chains in water and oil interfaces, respectively. Moreover, a characteristic time of ca. 10 ns is computed from both simulations as the time required for the dangling chains to migrate to the interfaces. The switchability of the surfaces is studied by simulating the system in cycles, such that the interface is changed from water to oil and back to water. The migration of HPI groups in the dangling chains towards water and back to bulk in oil (and vice versa) in each cycle is clearly shown by the simulations. A certain level of difference in the estimated properties can be expected for the

two methods due to the different nature in parameterization and resolution. Nevertheless, we can conclude that these methods agree with each reasonably well.

In conclusion, the simulations performed in this work help to understand the inherent nature of interactions, molecular structure, and segregation dynamics of a particular PU coating with dangling chains to maintain a targeted surface functionality. Moreover, the computational procedures as reported herein can be viewed as an important step towards establishing numerical tools in designing novel coatings. Our findings reveal a significant level of understanding of this particular coating, where the results can be extended to find applications in guiding the experimental studies.

Declaration of competing interest

The authors declare that they have no known competing financial interests or personal relationships that could have appeared to influence the work reported in this paper.

Data availability

Data will be made available on request.

Acknowledgments

Authors are thankful to the financial grant provided by TUBITAK and MSRT under the 2535 Bilateral Program (project no. 119N750). The DPD simulations reported in this paper are partially performed at TUBITAK ULAKBIM, High Performance and Grid Computing Center (TRUBA resources).

Appendix A. Supplementary data

Supplementary data to this article can be found online at https://doi.org/10.1016/j.porgcoat.2022.107279.

References

[1] O. Bayer, Das di-isocyanat-polyadditionsverfahren (polyurethane), Angew. Chem. 59 (2006) 257–272.
[2] D. Shen, S. Shi, T. Xu, X. Huang, G. Liao, J. Chen, Development of shape memory polyurethane based sealant for concrete pavement, Constr. Build. Mater. 174 (2018) 474–483.
[3] M. Adamczeski, in: Michael Szycher (Ed.), Szycher's Handbook of Polyurethanes, JOURNAL-AMERICAN CHEMICAL SOCIETY, 122, 2000, p. 3983.
[4] L. Jinze, L. Ma, G. Chen, Z. Zhou, Q. Li, High water-content and high elastic dual-responsive polyurethane hydrogel for drug delivery, J. Mater. Chem. B 3 (2015) 8401–8409.
[5] N.M.K. Lamba, K.A. Woodhouse, S.L. Cooper, Polyurethanes in Biomedical Applications, 1st ed., Routledge, 1998.
[6] E. Delebecq, J.-P. Pascault, B. Boutevin, F. Ganachaud, On the versatility ofurethane/urea bonds: reversibility, blocked isocyanate, and non-isocyanate polyurethane, Chem. Rev. 113 (2013) 80–118.
[7] K. Kojio, M. Furukawa, S. Matsumura, S. Motokucho, T. Osajima, K. Yoshinaga, The effect of cross-linking density and dangling chains on surface molecular mobility of network polyurethanes, Polym. Chem.-UK 3 (2012) 2287–2292.
[8] H. Ghermezcheshme, M. Mohseni, M. Ebrahimi, H. Makki, E. Martinelli, E. Guazzelli, S. Braccini, G. Galli, Effect of network topology on the protein adsorption behavior of hydrophilic polymeric coatings, ACS Appl.Polym.Mater. 4 (2021) 129–140.
[9] A.G. Tehrani, H. Makki, S.R.G. Anbaran, H. Vakili, H. Ghermezcheshme, N. Zandi, Superior anti-biofouling properties of mPEG-modified polyurethane networks via incorporation of a hydrophobic dangling chain, Prog. Org. Coat. 158 (2021), 106358.
[10] B.-S. Kim, C.E. Baez, A. Atala, Biomaterials for tissue engineering, World J. Urol. 18 (2000) 2–9.
[11] P.T.M. Albers, S.P.W. Govers, J. Laven, L.G.J. van der Ven, R.A.T.M. van Benthem, G. de With, A.C.C. Esteves, Design of dual hydrophobic-hydrophilic polymer networks for highly lubricious polyether-urethane coatings, Eur. Polym. J. 111 (2019) 82–94.
[12] T. Dikic, W. Ming, R.A.T.M. van Benthem, A.C.C. Esteves, G. de With, Self-replenishing surfaces, Adv. Mater. 24 (2012) 3701–3704.
[13] M. Yu, M. Liu, S. Fu, Slippery antifouling polysiloxane–polyurea surfaces with matrix self-healing and lubricant self-replenishing, ACS Appl. Mater. Interfaces 13 (27) (2021) 32149–32160.
[14] A.C.C. Esteves, K. Lyakhova, L.G.J. van der Ven, R.A.T.M. van Benthem, G. de With, Surface segregation of low surface energy polymeric dangling chains in a cross-linked polymer network investigated by a combined experimental-simulation approach, Macromolecules 46 (2013) 1993–2002.
[15] A.C.C. Esteves, K. Lyakhova, J.M. van Riel, L.G.J. van der Ven, R.A.T.M. van Benthem, G. de With, Self-replenishing ability of cross-linked low surface energy polymer films investigated by a complementary experimental-simulation approach, J. Chem. Phys. 140 (2014), 124902.
[16] K. Lyakhova, A.C.C. Esteves, M.W.P. van de Put, L.G.J. van der Ven, R.A.T.M. van Benthem, G. de With, Simulation-experimental approach to investigate the role of interfaces in self-replenishing composite coatings, Adv. Mater. Interfaces 1 (2014), 1400053.
[17] P. Szatkowski, K. Pielichowska, S. Blazewicz, Mechanical and thermal properties of carbon-nanotube-reinforced self-healing polyurethanes, J. Mater. Sci. 52 (2017) 12221–12234.
[18] Q. Tian, G. Yan, L. Bai, X. Li, L. Zou, L. Rosta, A. Wacha, Q. Li, I. Krakovský, M. Yan, Phase mixing and separation in polyester polyurethane studied by small-angle scattering: a polydisperse hard sphere model analysis, Polymer 147 (2018) 1–7.
[19] H. Makki, K.N. Adema, E.A. Peters, J. Laven, L.G. van der Ven, R.A. van Benthem, G. de With, Degradation of a polyester-urethane coating: physical properties, J. Polym. Sci. B Polym. Phys. 54 (2016) 659–671.
[20] P. Schön, K. Bagdi, K. Molnár, P. Markus, B. Pukánszky, G.J. Vancso, Quantitative mapping of elastic moduli at the nanoscale in phase separated polyurethanes by AFM, Eur. Polym. J. 47 (2011) 692–698.
[21] E. Iype, A. Esteves, G. de With, Mesoscopic simulations of hydrophilic cross-linked polycarbonate polyurethane networks: structure and morphology, Soft Matter 12 (2016) 5029–5040.
[22] G. Kacar, P. Albers, A. Esteves, G. de With, Mesoscopic structure and swelling properties of crosslinked polyethylene glycol in water, J. Coat. Technol. Res. 15 (2018) 691–701.
[23] G. Kacar, E.A. Peters, G. de With, Multi-scale simulations for predicting material properties of a cross-linked polymer, Comp. Mater. Sci. 102 (2015) 68–77.
[24] G. Kacar, E.A. Peters, G. de With, Structure of a thermoset polymer near an alumina substrate as studied by dissipative particle dynamics, J. Phys. Chem. C 117 (2013) 19038–19047.
[25] H. Makki, K.N. Adema, E.A. Peters, J. Laven, L.G. van der Ven, R.A. van Benthem, G. de With, Multi-scale simulation of degradation of polymer coatings: thermo-mechanical simulations, Polym.Degrad.Stab. 123 (2016) 1–12.
[26] H. Makki, K.N. Adema, E.A. Peters, J. Laven, L.G. van der Ven, R.A. van Benthem, G. de With, A simulation approach to study photo-degradation processes of polymeric coatings, Polym.Degrad.Stab. 105 (2014) 68–79.
[27] M. Azimi, S.S. Mirjavadi, A.M.S. Hamouda, H. Makki, Heterogeneities in polymer structural and dynamic properties in graphene and graphene oxide nanocomposites: molecular dynamics simulations, Macromol.Theory Simul. 26 (2017), 1600086.
[28] I. Jiménez-Pardo, L.G. Van der Ven, R.A. Van Benthem, G. de With, A.C.C. Esteves, Hydrophilic self-replenishing coatings with long-term water stability for anti-fouling applications, Coatings 8 (2018) 184.
[29] F. Karasu, C. Rocco, Y. Zhang, C. Croutxé-Barghorn, X. Allonas, L. van der Ven, R. van Benthem, A. Esteves, LED-cured self-replenishing hydrophobic coatings based on interpenetrating polymer networks (IPNs), RSC Adv. 6 (2016) 33971–33982.
[30] Y. Wang, L.M. Pitet, J.A. Finlay, L.H. Brewer, G. Cone, D.E. Betts, M.E. Callow, J. A. Callow, D.E. Wendt, M.A. Hillmyer, Investigation of the role of hydrophilic chain length in amphiphilic perfluoropolyether/poly (ethylene glycol) networks: towards high-performance antifouling coatings, Biofouling 27 (2011) 1139–1150.
[31] Y. Zhang, F. Karasu, C. Rocco, L. van der Ven, R. van Benthem, X. Allonas, C. Croutxe-Barghorn, A. Esteves, G. de With, PDMS-based self-replenishing coatings, Polymer 107 (2016) 249–262.
[32] Z. Wang, H. Zuilhof, Self-healing fluoropolymer brushes as highly polymer-repellent coatings, J. Mater. Chem. A 4 (2016) 2408–2412.
[33] H. Tanoue, M. Inutsuka, N.L. Yamada, K. Ito, H. Yokoyama, Kinetics of dynamic polymer brush formation, Macromolecules 50 (2017) 5549–5555.
[34] P. Español, P. Warren, Statistical-mechanics of dissipative particle dynamics, Europhys. Lett. 30 (1995) 191–196.
[35] P. Español, P.B. Warren, Perspective: dissipative particle dynamics, J. Chem. Phys. 146 (2017), 150901.
[36] R.D. Groot, P.B. Warren, Dissipative particle dynamics: bridging the gap between atomistic and mesoscopic simulation, J. Chem. Phys. 107 (1997) 4423–4435.
[37] S.J. Marrink, H.J. Risselada, S. Yefimov, D.P. Tieleman, A. De Vries, The MARTINI force field: coarse grained model for biomolecular simulations, J. Phys. Chem. B 111 (2007) 7812–7824.
[38] G. Kacar, E.A.J.F. Peters, G. de With, Mesoscopic simulations for the molecular and network structure of a thermoset polymer, Soft Matter 9 (2013) 5785–5793.
[39] H. Ghermezcheshme, H. Makki, M. Mohseni, M. Ebrahimi, G. de With, MARTINI-based simulation method for step-growth polymerization and its analysis by size exclusion characterization: a case study of cross-linked polyurethane, Phys. Chem. Chem. Phys. 21 (2019) 21603–21614.
[40] H. Ghermezcheshme, H. Makki, M. Mohseni, M. Ebrahimi, Hydrophilic dangling chain interfacial segregation in polyurethane networks at aqueous interfaces and its underlying mechanisms: molecular dynamics simulations, Phys. Chem. Chem. Phys. 22 (2020) 26351–26363.

[41] P.J. Hoogerbrugge, J.M.V.A. Koelman, Simulating microscopic hydrodynamic phenomena with dissipative particle dynamics, Europhys. Lett. 19 (1992) 155–160.
[42] U. Frisch, B. Hasslacher, Y. Pomeau, Lattice-gas automata for the Navier-Stokes equation, Phys. Rev. Lett. 56 (1986) 1505–1508.
[43] P.J. Flory, Principles of Polymer Chemistry, Cornell University Press, Ithaca, New York, 1953.
[44] M.B. Liu, G.R. Liu, L.W. Zhou, J.Z. Chang, Dissipative particle dynamics (DPD): an overview and recent developments, Arch. Comput. Method E 22 (2015) 529–556.
[45] G. Kacar, E.A.J.F. Peters, G. de With, A generalized method for parameterization of dissipative particle dynamics for variable bead volumes, Europhys. Lett. 102 (2013) 40009.
[46] G. Kacar, Characterizing the structure and properties of dry and wet polyethylene glycol using multi-scale simulationst, Phys. Chem. Chem. Phys. 20 (2018) 12303–12311.
[47] G. Kacar, Dissipative particle dynamics parameterization and simulations to predict negative volume excess and structure of PEG and water mixtures, Chem. Phys. Lett. 690 (2017) 133–139.
[48] G. Kacar, G. de With, Hydrogen bonding in DPD: application to low molecular weight alcohol–water mixtures, Phys. Chem. Chem. Phys. 18 (2016) 9554–9560.
[49] G. Kacar, G. de With, Parametrizing hydrogen bond interactions in dissipative particle dynamics simulations: the case of water, methanol and their binary mixtures, J. Mol. Liq. 302 (2020), 112581.
[50] G. Kacar, Molecular understanding of interactions, structure, and drug encapsulation efficiency of pluronic micelles from dissipative particle dynamics simulations, Colloid Polym. Sci. 297 (2019) 1037–1051.
[51] S.J. Marrink, A.H. De Vries, A.E. Mark, Coarse grained model for semiquantitative lipid simulations, J. Phys. Chem. B 108 (2004) 750–760.
[52] F.A. Herzog, L. Braun, I. Schoen, V. Vogel, Improved side chain dynamics in MARTINI simulations of protein–lipid interfaces, J. Chem. Theory Comput. 12 (2016) 2446–2458.
[53] C.A. López, A.J. Rzepiela, A.H. de Vries, L. Dijkhuizen, P.H. Hünenberger, S. J. Marrink, Martini coarse-grained force field: extension to carbohydrates, J. Chem. Theory Comput. 5 (2009) 3195–3210.
[54] J.J. Uusitalo, H.I. Ingólfsson, P. Akhshi, D.P. Tieleman, S.J. Marrink, Martini coarse-grained force field: extension to DNA, J. Chem. Theory Comput. 11 (2015) 3932–3945.
[55] J. Zavadlav, M.N. Melo, A.V. Cunha, A.H. De Vries, S.J. Marrink, M. Praprotnik, Adaptive resolution simulation of MARTINI solvents, J. Chem. Theory Comput. 10 (2014) 2591–2598.
[56] G. Rossi, L. Monticelli, S.R. Puisto, I. Vattulainen, T. Ala-Nissila, Coarse-graining polymers with the MARTINI force-field: polystyrene as a benchmark case, Soft Matter 7 (2011) 698–708.
[57] G. Rossi, I. Giannakopoulos, L. Monticelli, N.K. Rostedt, S.R. Puisto, C. Lowe, A. C. Taylor, I. Vattulainen, T. Ala-Nissila, A MARTINI coarse-grained model of a thermoset polyester coating, Macromolecules 44 (2011) 6198–6208.
[58] H. Vakili, M. Mohseni, H. Makki, H. Yahyaei, H. Ghanbari, A. Gonzalez, L. Irusta, Synthesis of segmented polyurethanes containing different oligo segments: experimental and computational approach, Prog.Org.Coat. 150 (2021), 105965.
[59] H. Vakili, M. Mohseni, H. Makki, H. Yahyaei, H. Ghanbari, A. González, L. Irusta, Microphase arrangement of smart superhydrophilic segmented polyurethanes at their Interface with water, Langmuir 36 (2020) 13201–13209.
[60] H. Vakili, M. Mohseni, H. Makki, H. Yahyaei, H. Ghanbari, A. González, L. Irusta, Self-assembly of a patterned hydrophobic-hydrophilic surface by soft segment microphase separation in a segmented polyurethane: combined experimental study and molecular dynamics simulation, Polymer 195 (2020), 122424.
[61] H. Hasheminejad, S. Herziger, A. Mirzaalipour, A.K. Singh, R.R. Netz, C. Böttcher, H. Makki, S.K. Sharma, R. Haag, Supramolecular engineering of alkylated, fluorinated, and mixed amphiphiles, Macromol. Rapid Commun. 2100914 (2022).
[62] S. Plimpton, Fast parallel algorithms for short-range molecular dynamics, J. Comput. Phys. 117 (1995) 1–19.
[63] F. Grunewald, G. Rossi, A.H.De Vries, S.J. Marrink, L. Monticelli, Transferable MARTINI model of poly (ethylene oxide), J. Phys. Chem. B 122 (2018) 7436–7449.